IMPROVING HEAVY VEHICLE EMERGENCY BRAKING SYSTEMS

Jonathan Miller is a graduate of the University of Calgary, 2003. He completed a Master's degree at McGill University in 2006. He is currently working towards a PhD in engineering at Cambridge University with a focus on advanced heavy vehicle braking systems.

David Cebon is Professor of Mechanical Engineering at Cambridge University. He is a Fellow of the Royal Academy of Engineering, the Director of the Cambridge Vehicle Dynamics Consortium, and the Managing Director of Granta Design Limited.

J. Miller
Cambridge University
United Kingdom

D. Cebon
Cambridge University
United Kingdom

Abstract

This paper introduces a sliding mode braking force observer to support a sliding mode controller for air-braked heavy vehicles. The performance of the observer is examined through simulations and field testing of an articulated heavy vehicle. The observer was found to operate robustly during single-wheel vehicle simulations, and provide reasonable estimates of surface friction from test data. The effect of brake gain errors on the controller and observer are illustrated, and a recursive least squares estimator is derived for the brake gain. The estimator converged within 0.3 s in simulations and vehicle trials.

Keywords: emergency braking system; pneumatic actuators; parameter estimation; state estimation

1. Introduction

Heavy Goods Vehicles (HGV's) have considerably lower maximum retardation rates than passenger cars (Werde and Decker, 1992), contributing to their higher rate of involvement in fatal accidents than any other road vehicles (Annon., 2006, Peeta et al., 2005). The mandatory use of anti-lock braking systems (ABS) on air braked vehicles in Europe has mitigated this problem somewhat. However, current HGV ABS systems use heuristic control approaches that work on cycles of predicting and superseding the limits of tyre-road adhesion, and then reducing the brake pressure to allow the wheel to rotate again (Kienhofer and Cebon, 2004). When considering a typical wheel slip vs. braking force curve (Figure 1), the periodic locking and unlocking of the wheel substantially reduces the average braking force compared with the desired value at the peak of the curve. In addition, the pneumatic chamber fill and dump process uses a lot of air, which requires energy to generate and large reservoirs for storage.
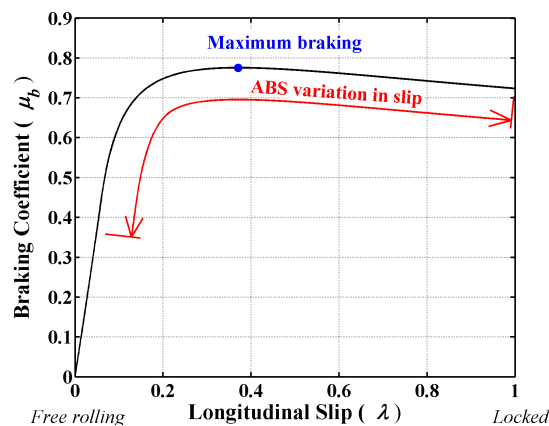
Figure 1 – Braking coefficient (longitudinal tyre force / vertical tyre force) vs. longitudinal slip on asphalt

An alternative approach to ABS is wheel slip control, which optimizes wheel slip continuously during braking, thereby maximizing deceleration while maintaining vehicle maneuverability. Preliminary estimations with a proof-of-concept control system and vehicle simulation predict reductions of up to 35% in braking distance relative to conventional ABS (Miller et al., 2008a). Moreover, since only small adjustments are made to keep the wheel at the optimum slip point, slip control can also reduce compressed air consumption.

To achieve these benefits, the bandwidth of the pneumatic system must be increased substantially. It has been shown in Miller et al. (2008a, 2008b) that actuation delays in heavy vehicles could be reduced by an order of magnitude by placing fast pneumatic valves directly on brake chambers. Such reductions in actuation delay would allow advanced braking control methods to be used on pneumatically braked vehicles.

In general, however, advanced control methods require knowledge of the slip-friction characteristics of the tyre-road system. This is impractical to measure directly and must be estimated. Past studies on tyre force estimation have focused on estimators for cars (Ray, 1997, Hodgson and Best, 2006, Unsal and Kachroo, 1999, Drakunov et al., 1995). Heavy

vehicles have very different tyre characteristics and dynamic behaviour to cars, and so represent a significantly different estimation problem. Only Ribbens et al. (2007) and Patel et

al. (2008) designed observers specifically for trucks. Neither of these investigations included experimental results. The purpose of this paper is to introduce an advanced braking control algorithm for HGV's, to discuss the estimation algorithms necessary to support the controller, and to supplement the discussion with experimental results.

2.   System Model

A 'quarter-car' braking simulation was used during control system design. The simulation has four degrees of freedom (see Figure 2): longitudinal motion of the vehicle, rotational motion of the wheel, and vertical motion of the sprung and unsprung masses. The longitudinal motion of the vehicle in the simulation is described by

$$F_x + m_v \dot{v}_x = 0 \tag{1}$$

where F_x is the longitudinal tyre force (braking force), m_v is the total vehicle mass, and v_x is the longitudinal velocity of the vehicle. The rotational speed of the wheel, ω, is related to the braking torque, T_B, and the braking force by

$$J\dot{\omega} - rF_x + T_B = 0 \tag{2}$$

with r being the radius through which the braking force acts. It is assumed that braking torque is proportional to the pressure in the brake chamber, P_c, and that disc brakes are used, so brake fade can be neglected (Radlinski, 2007). Hence,

$$T_B = GP_c \tag{3}$$

where G is called the "brake gain."

The vertical dynamics of the vehicle is described by

$$\begin{bmatrix} m_s & 0 \\ 0 & m_u \end{bmatrix}\begin{bmatrix} \ddot{z}_s \\ \ddot{z}_u \end{bmatrix} + \begin{bmatrix} c_s & -c_s \\ -c_s & c_s + c_t \end{bmatrix}\begin{bmatrix} \dot{z}_s \\ \dot{z}_u \end{bmatrix} + \begin{bmatrix} k_s & -k_s \\ -k_s & k_s + k_t \end{bmatrix}\begin{bmatrix} z_s \\ z_u \end{bmatrix} = \begin{bmatrix} 0 \\ c_t\dot{z}_r + k_tz_r \end{bmatrix} \tag{4}$$

where m, c, and k denote mass, stiffness, and damping respectively; z is displacement; and the subscripts 't', 'r', 'u', and 's' denote the tyre, road, unsprung, and sprung masses respectively. The vehicle model was subjected to road surface roughness with specified spectral content corresponding to the ISO classification 8608:1995 (Annon., 1995), and quantified by the International Road Roughness Index (IRI) (Sayers and Gillespie, 1986). A semi-empirical truck tyre model from the University of Michigan Transportation Research Institute (UMTRI) was used to calculate the braking forces based on the wheel slip, λ, defined as (Fancher, 1995)

$$\lambda = \frac{v_x - r_r\omega}{v_x} \tag{5}$$

where r_r is the rolling radius of the wheel.
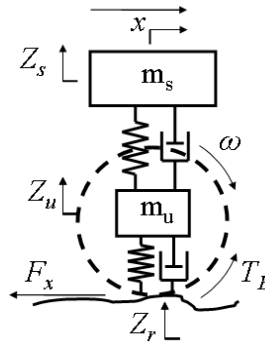
Figure 2 – Quarter car vehicle model

Brake chamber charging and discharging dynamics were described using one-dimensional flow theory and thermodynamic relations for unsteady flow through an open system. The governing equations are omitted here for brevity, and can be found in Miller et al. (2008b). It was assumed that pulse-width modulated valves were used to control flow into and out of the chamber via linear pressure control.

3. Sliding Mode Slip Controller

A variable structure "sliding mode" approach was taken for the slip control problem, since variable structure controllers are robust and can handle unstable, nonlinear plants. The derivation of the controller can be found in Miller et al. (2008a), with the final expression given by:

$$P_c = \frac{r_r r F_x - (1 - \lambda)\dot{v}_x J}{2Gr_r} - k_s \left\{ \frac{s}{|s| + \delta} \right\} - \Phi s \qquad (6)$$

$$s = \lambda_d - \lambda$$

where k_c, Φ, and δ are positive design constants, s is the sliding surface, and λ_d is the desired slip. The controller gains were tuned for given actuator speeds to optimize performance and energy usage. Further details of this tuning can be found in Miller et al. (2008a).

Figure 3 shows the slip and chamber pressure time histories for a simulated stop using the sliding mode controller on a rough (IRI = 20 m/km), high friction ($\mu = 0.9$) surface. A valve delay of 1 ms, which is the lowest practical delay possible for pneumatic brakes (Miller et al., 2008a), was used for the simulations. The demand slip was set as the optimal slip point for a given road friction level, and increases as the vehicle slows to account for the velocity dependence of the tyre curves in the UMTRI model (Fancher, 1995). Keeping in line with industry practice, the brakes are fully depressed in the simulation once the vehicle speed drops below 2 m/s.

The speed of the valve allows the chamber pressure to respond to fast changes in the pressure demand signal. Consequently, the control system rejects the road roughness, causing the rapid variation in chamber pressure in Figure 3 b), and accurately regulates the wheel slip to the demand signal in Figure 3 a). In general, it was found that the vehicle stopped more than 30%

shorter in simulations with slip control when compared to conventional ABS algorithms and hardware (Miller et al., 2008a).

| a) Slip Time History | b) Chamber Pressure Time History |
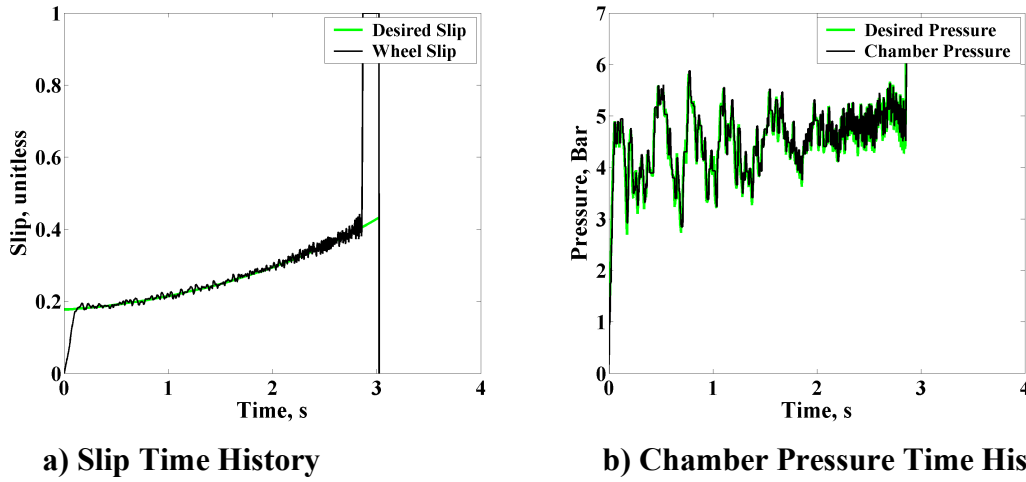
Figure 3 – Simulated sliding mode slip controlled stop on a high friction, rough road (μ = 0.9, IRI = 20 m/km)

4. Friction Force Observer

4.1 Observer Equations

The results in Figure 3 are encouraging, but the controller uses states that are impractical to measure, such as the tyre force F_x. Consequently, it is necessary to derive a friction force observer. A sliding mode observer was chosen here to estimate the tyre tractive forces since, unlike Kalman filters, sliding observers have stability guarantees and are robust to model mismatches (Edwards and Spurgeon, 1998, Misawa and Hedrick, 1989). Using standard state space notation, the governing equations for the sliding mode observer may be written as

$$\dot{\hat{x}} = A\hat{x} + Bu + L(y - \hat{y}) + k_o \, \mathrm{sgn}(y - \hat{y})$$
$$y = Cx$$
(7)

where L and k_o are design gains, and '^' denotes an estimate.

Tyre slip-friction curves change on different surfaces and as the tyre wears. Consequently, it was decided to follow Ray (1997) and treat the tyre forces as unknown parameters to be estimated, rather than assuming a tyre model in advance. The longitudinal force was modeled using a random walk, and it was assumed that the wheel speed, longitudinal acceleration, and chamber pressure can be measured. Based on this, the state equations for the system are

$$\dot{x} = \begin{bmatrix} \dot{\omega} \\ \dot{F}_x \\ \ddot{F}_x \end{bmatrix} = \begin{bmatrix} 0 & \dfrac{r}{J} & 0 \\ 0 & 0 & 1 \\ 0 & 0 & 0 \end{bmatrix} \begin{bmatrix} \omega \\ F_x \\ \dot{F}_x \end{bmatrix} + \begin{bmatrix} -\dfrac{2G}{J} \\ 0 \\ 0 \end{bmatrix} P_c$$
(8)

$$y = \begin{bmatrix} \dot{v}_x \\ \omega \end{bmatrix} = \begin{bmatrix} 0 & -\dfrac{1}{m_v} & 0 \\ 1 & 0 & 0 \end{bmatrix} \begin{bmatrix} \omega \\ F_x \\ \dot{F}_x \end{bmatrix}$$

From Equation (8), it can be seen that the system is observable without the accelerometer as an output. However, accelerometers are commonly available in commercial emergency braking systems, so it was of interest to explore whether the extra information from this sensor would improve the efficacy of the observer.

4.2 Observer Results

Band-limited white noise with a sample time of 0.002 s was added to the wheel speed and acceleration signals in the simulations when evaluating the sliding mode observer. The amplitude of the noise was tuned to emulate measurements taken during braking tests with a full-scale vehicle (Kienhofer and Cebon, 2004). Accelerometer bias, however, was omitted, since algorithms exist to estimate this online (Bevly, 2007).

The observer gains, L and k_o, were initially calculated using the pole placement method detailed by Edwards and Spurgeon (1998). The relative weightings for each state in the observer were then tuned iteratively with respect to wheel speed and longitudinal acceleration measurements to obtain the best results. Figure 4 shows a simulation of the observer's performance "in-the-loop" on a rough, high friction surface. The observer accurately tracks the "true" tyre forces, responding quickly to changes in force levels, and the controller is able to precisely track the target slip.

| a) Slip Time History | b) Tyre Force Time History |
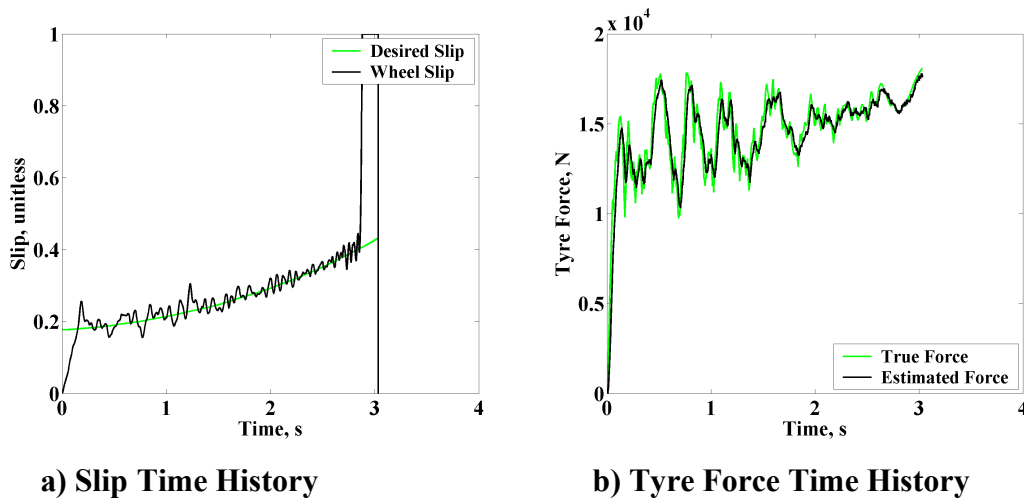
Figure 4 – Simulated sliding mode observer performance on a high friction, rough road (μ = 0.9, IRI = 20 m/km)

4.3 Multi-Wheeled Models

A six-wheeled vehicle model, simulating an entire semi-trailer, was derived such that

$$\sum_{i=1}^{6} F_{x_i} + m_v \dot{v}_x = 0 \tag{9}$$

where i represents the wheel number, and m_v includes the weight of the tractor. Each individual wheel has the dynamics described by Equations (2) – (5) and is controlled by a sliding controller described by Equation (6). The sliding mode observer was extended for the 6-wheeled model assuming the 6 wheel speeds, chamber pressures, and vehicle longitudinal acceleration were measured. The observer states and measured variables were expanded as

$$\dot{x} = \begin{bmatrix} \dot{\omega}_1 & \dot{\omega}_2 & \dot{\omega}_3 & \dot{\omega}_4 & \dot{\omega}_5 & \dot{\omega}_6 & \dot{F}_{x_1} & \dot{F}_{x_2} & \dot{F}_{x_3} & \dot{F}_{x_4} & \dot{F}_{x_5} & \dot{F}_{x_6} & \ddot{F}_{x_1} & \ddot{F}_{x_2} & \ddot{F}_{x_3} & \ddot{F}_{x_4} & \ddot{F}_{x_5} & \ddot{F}_{x_6} \end{bmatrix}^T \quad (10)$$
$$y = \begin{bmatrix} \dot{v}_x & \omega_1 & \omega_2 & \omega_3 & \omega_4 & \omega_5 & \omega_6 \end{bmatrix}^T$$

where the subscripted '1-6' denotes the wheel number, and the braking force on each wheel was modeled similarly to Equation (8). The observer gains were tuned similarly to the single-wheel case.

The observer was evaluated experimentally using an instrumented semi-trailer fitted with wide single tyres and conventional ABS, and towed by a Volvo FH12 (2-axle) tractor. The vehicle was tested in the laden condition, with a gross vehicle weight of approximately 38 t. Brake chamber pressure, pressure demand, and wheel speeds were logged at 100 Hz at each of the 6 trailer wheels, as was the longitudinal and lateral acceleration, and the longitudinal speed of the trailer. The test procedure involved accelerating the vehicle to the test speed of 50 km/h, disengaging the clutch, and electronically sending a pressure demand of 6.5 bar (equivalent to an emergency stop) to the trailer ABS ECUs. Tests were run at the MIRA proving ground on a "wet basalt tile" track with a nominal friction of $\mu = 0.2$ (Ashley and MacKellar, 1985). The track had only small amounts of roughness. All vehicle parameters, such as brake gain and wheel radius, were known approximately during post processing of the measured data.

The effectiveness of the observer for the three offside trailer wheels is shown in Figure 5. The estimated slip curves traced out by the wheels during the stop are shown in Figure 5 b). The true force time histories are not available for comparison. However, the level of tyre-road friction predicted by the observer is close to the value specified for the track, with the discrepancy thought to be caused by the near-freezing air temperature during the tests. Moreover, the tractive forces of the three wheels encouragingly collapsed on each other, and the slip curves traced out have reasonable shapes. The scatter of data in Figure 5 b) is likely caused by sensor noise, variability in the actual surface friction, and the velocity dependence of the tyre force characteristics.
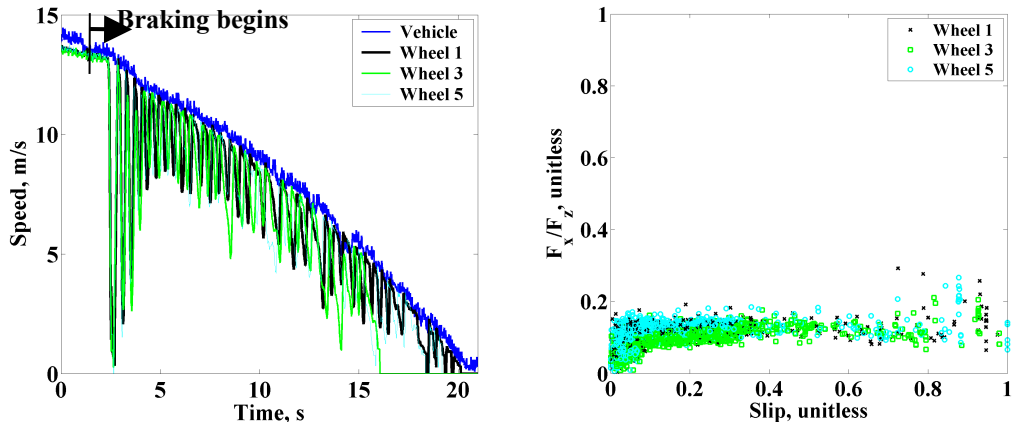
a) Speed time histories   b) Slip curve traced out during the stop

Figure 5 – Measured sliding mode observer performance on a low friction, wet basalt tile surface (μ = 0.2) with conventional ABS

4.4 Observer Robustness

A problem frequently neglected in the literature is the robustness of tractive force observers to brake gain errors. Brake gains can vary by over 30% per brake due to manufacturing variations, ageing, moisture, stopping history, etc. (Radlinski, 2007). Since the brake gain is multiplicative to the input in Equation (8), errors in the gain directly affect the information that is being used for estimation.

Figure 6 a) shows the performance of the sliding mode force observer on the single-wheel model with a 50% brake gain error in the algorithm and measurement of the wheel speed only. There is a corresponding 50% error in the estimated force. Figure 6 b) shows the performance of the observer with the same brake gain error and the longitudinal acceleration measured as well. The observer was not in the control loop for either simulation run. Since vehicle acceleration is directly related to braking force through Equation (1), the accelerometer significantly improves the accuracy of the estimator.

Unfortunately, the theoretical benefit of the additional accelerometer measurements is only available for a single-wheeled vehicle, where Equation (1) holds. For a real heavy vehicle with multiple axles, Equation (9) applies instead. In this case, there are an infinite number of possible combinations of brake gains that can generate the measured longitudinal acceleration, and the observer does not have sufficient information to estimate each one accurately.

a) Measuring only ω

b) Measuring ω and a$_x$
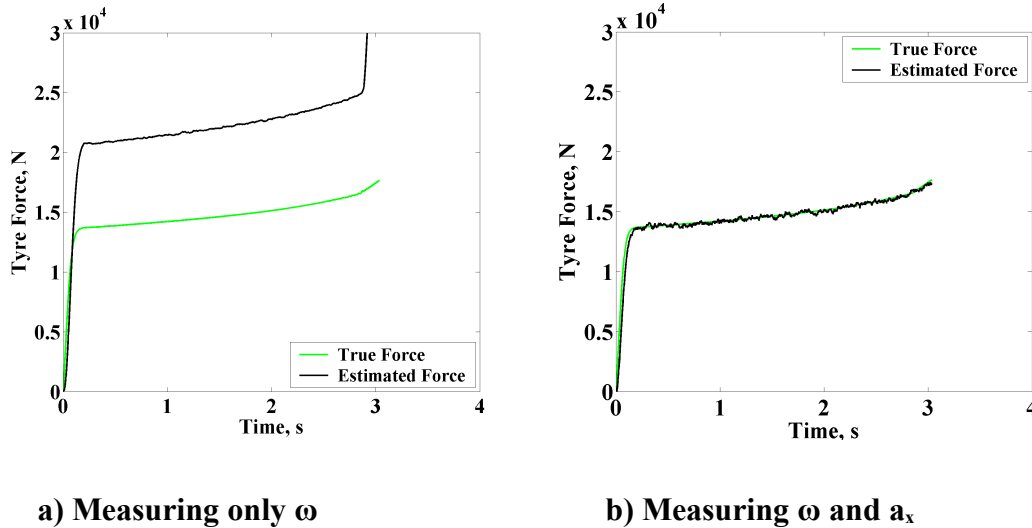
Figure 6 – Simulated sliding mode observer performance with a 50% error in brake gain (μ = 0.9, IRI = 0 m/km)

Figure 7 shows the performance of the nominal sliding observer on the six-wheeled model and a high friction, smooth road with brake gain variations ranging between 20% and 50% on each wheel of the vehicle. The brake gains are intentionally allowed to affect the sliding mode controller. The observer interprets Equation (9) to mean that the braking forces on all wheels are approximately the same and equal to the average of the set, as can be seen in Figures 7 a) and b), whereas this is clearly not the case in Figure 7 c). The observer gains, k_o and L can be tuned so that the estimation relies more on the individual wheel speeds than the accelerometer measurements, but inaccuracies will ensue as in the case of Figure 6 a) due to the brake gain errors. Consequently, it is necessary to estimate the individual brake gains.

| a) Forces on Wheel 1 | b) Forces on Wheel 4 | c) Slip on All Wheels |
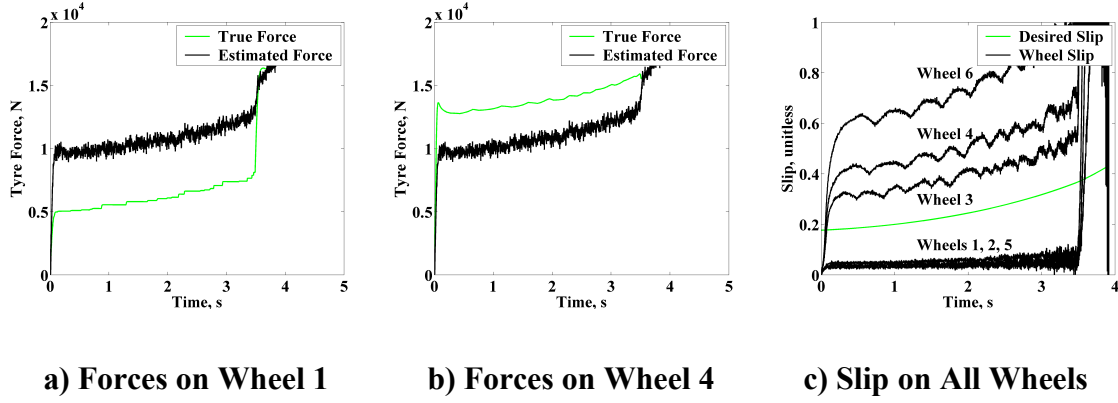
Figure 7 – Simulated sliding mode observer performance on a 6-wheeled model and a smooth, high friction surface (μ = 0.9, IRI = 0 m/km) with brake gain errors ranging between 20-50%

5. Brake Gain Estimation

5.1 Estimation Algorithm Equations

The observable system described by Equation (8) cannot be used as a parameter identifying observer by augmenting it with the brake gain as a state, without adding more measured variables. Since all critical variables related to braking are already being used as inputs or measured states, an alternative approach to brake gain estimation was explored. The proposed algorithm estimates the brake gains before emergency braking, so they can be used at the start of the braking event. The procedure involves a short, strong application of the brake on each wheel in turn during free rolling. In this way, the braking force is directly related to the vehicle deceleration. A least squares approach can then be used to estimate the brake gain.

Rearranging Equation (2) to linearly parameterize the brake gain against the other variables,

$$y = 1 \cdot G = \frac{-rm_v \dot{v}_x - J\dot{\omega}}{P_c} \tag{11}$$

Following the standard recursive least squares formulation (Kiencke and Nielsen, 2000), the brake gain estimator is given by,

$$\hat{G}(n) = \hat{G}(n-1) + k_e(n)\left[y(n) - 1 \cdot \hat{G}(n-1)\right] \tag{12}$$

$$k_e(n) = \frac{P(n-1)}{\varphi + P(n-1)}$$

$$P(n) = \frac{P(n-1)}{\varphi} - \frac{k_e(n)P(n-1)}{\varphi}$$

where n is a given time step, k_e is the recursive gain, P is the covariance matrix, and φ is the forgetting factor.

5.2 Estimator Results

Figure 8 shows the effectiveness of the estimator in simulations on a medium friction, rough road. The six-wheeled simulation featuring sensor noise was used and a brake demand of 2 bar was sent to the leading offside wheel for 0.3 s, starting 0.5 s into the simulation. Despite the noise and roughness, the algorithm quickly estimated the correct brake gain. The variability seen in Figure 8 b) is caused by instantaneous biases in the sensor noise.

a) Vehicle and Wheel Speeds   b) Gain Estimation on Wheel 1
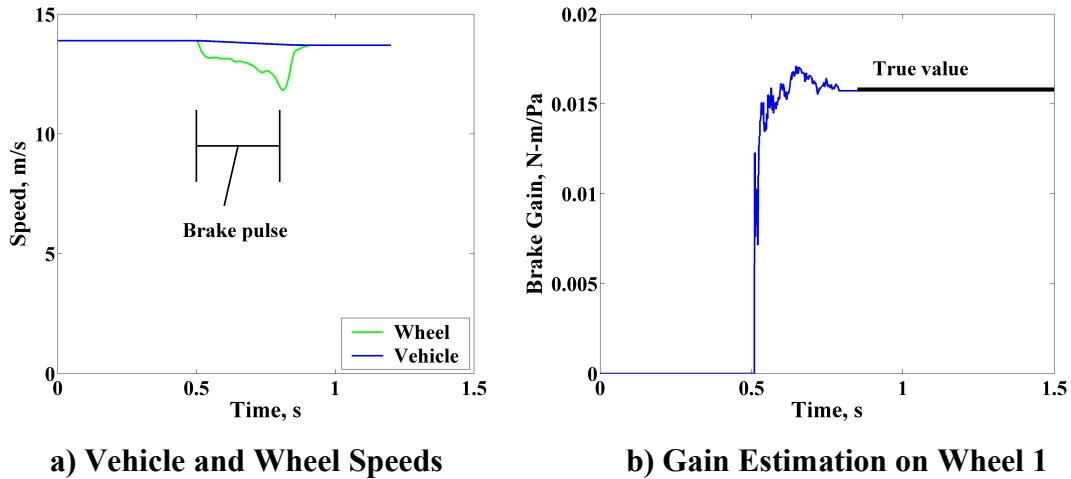
Figure 8 – Simulated brake pulse used for brake gain estimation on a medium friction, rough road (μ = 0.4, IRI = 20 m/km) with sensor noise

The brake gain estimation algorithm was tested on the tractor semi-trailer described in Section 4.2. The vehicle was unladen and had a total weight of approximately 20 t. The test procedure involved accelerating the vehicle to the test speed of 50 km/h on a high friction, slightly rough road, disengaging the clutch, and electronically sending a pressure demand pulse to the ABS ECUs for each trailer wheel in succession. The width and magnitude of the pulses were increased to 0.5 s and 3 bar respectively, to enhance the clarity of the results.

a) Vehicle and Wheel Speeds   b) Gain estimation on wheel 4
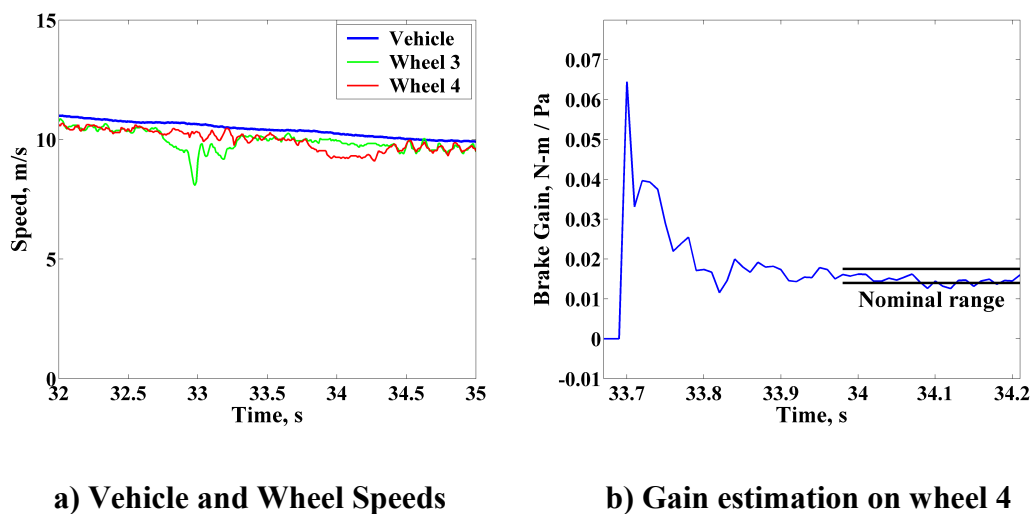
Figure 9 – Measured brake gain estimation during vehicle tests on a high friction, mildly rough road

Estimation results for a sample run are shown in Figure 9. Accelerometer readings were compared to those at the beginning of a test run, so the accelerometer bias could be removed. The brake gain of the vehicle was expected to be in the range of 0.014-0.017 N-m/Pa, based on manufacturer information and previous tests. The estimator converged to plausible values within 0.3 s, with the estimated value varying by only 10% after convergence. The estimator was not, however, consistent throughout all the runs. The data acquisition could only be run at 100 Hz, and the coarseness of the data points caused slow and unreliable convergence for some runs. Further vehicle tests are planned with 500 Hz sampling to prove the reliability of the estimator.

6. Conclusions

(i) A sliding mode controller was presented for a pneumatically braked vehicle, and was shown to precisely control slip on rough roads in simulations.

(ii) A sliding mode braking force observer was derived assuming a random walk model for the force and using measurements of longitudinal vehicle acceleration, wheel speed, and brake pressure.

(iii) The sliding mode observer gave accurate results in simulations. The observer performed well in vehicle tests, approximately predicting the road friction level.

(iv) While the accelerometer made the observer robust to brake gain errors in single-wheeled vehicles, the result does not hold for multi-wheeled vehicles.

(v) A brake gain estimator was derived using the recursive least squares algorithm to supplement the sliding controller and observer. It requires pulsing each brake in turn during free-wheeling.

(vi) Brake gains were estimated with reasonable accuracy during simulations and gave promising values in vehicle tests.

References

- Werde, J. and Decker, H. (1992), "Brake by Wire for Commercial Vehicles," Trans. of SAE, 922489, 849-859.
- Annon. (2006), "Traffic Safety Facts, 2005" National Highway Traffic and Safety Administration, US Department of Transportation, 1-222.
- Peeta, S., Zhang, P. and Zhou, W. (2005), "Behavior-Based Analysis of Freeway Car-Truck Interactions and Related Mitigation Strategies," Transportation Research Part B – Methodological, 39, 5, 417-451.
- Kienhofer, F. and Cebon, D. (2004), "An Investigation of ABS Strategies for Articulated Vehicles" in Proc. of the 8th International Symposium on Heavy Vehicle Weights and Dimensions, 1-15.

- Miller, J., Kienhofer, F. and Cebon, D. (2008), "The Design and Evaluation of an Alternative Heavy Vehicle Braking System" in Proc. Of the 9th International Symposium on Advanced Vehicle Control, Kobe, Japan.
- Miller, J., Kienhofer, F. and Cebon, D. (2008), "Design Concept for an Alternative Heavy Vehicle Slip Control Brake Actuator" in Proc. of the 10th International Symposium on Heavy Vehicle Transport Technology, 429-442.
- Ray, L., R. (1997), "Nonlinear Tire Force Estimation and Road Friction Identification: Simulation and Experiments," Automatica, 33, 10, 1819-1833.
- Hodgson, G. and Best, M.C. (2006), "A Parameter Identifying a Kalman Filter Observer for Vehicle Handling Dynamics," Proc. of the IMECHE Part D – Journal of Automobile Engineering, 220, D8, 1063-1072.
- Unsal, C. and Kachroo, P. (1999), "Sliding Mode Measurement Feedback Control for Antilock Braking Systems," IEEE Transactions on Control Systems Technology, 7, 2, 271-281.
- Drakunov, S., Ozguner, U., Dix, P. and Ashrafi, B. (1995), "ABS Control Using Optimum Search via Sliding Modes," IEEE Transactions on Control Systems Technology, 3, 1, 79-85.
- Ribbens, W.B., Ribbens, J.A. and Fredricks, R. (2007), "Sliding Mode Observer-Based ABS Offers Advantages for HD Truck Applications" in Proc. of the SAE 2007 Commercial Vehicle Engineering Congress & Exhibition, 2007-01-4243, 1-8.
- Patel, N., Edwards, C. and Spurgeon, S.K. (2008), "Tyre-Road Friction Estimation – A Comparative Study," Proc. of the IMECHE Part D – Journal of Automobile Engineering, 222, 12, 2337-2351.
- Radlinski, D., (2007), "Mechanics of Heavy Duty Truck Systems Course Notes – Braking Capabilities of Heavy-Duty Trucks" UMTRI Course on Heavy Vehicle Systems, Cambridge University Engineering Department, Cambridge, UK.
- Annon., (1995) "Mechanical Vibration – Road Surface Profiles – Reporting of Measured Data" ISO 8608:1995, International Organization for Standardization.
- Sayers, M. and Gillespie, T. (1986) "Guidelines for Conducting and Calibrating Road Roughness Measurements" University of Michigan Transportation Research Institute, 1-96.
- Fancher, P.S. (1995) "Generic Data for Representing Truck Tire Characteristics in Simulations of Braking and Braking-in-a-Turn Maneuvers" University of Michigan Transportation Research Institute, 1-103.
- Slotine, J.J. and Li, W. (1991), Applied Nonlinear Control, Prentice-Hall Inc., Englewood Cliffs, NJ.
- Edwards, C. and Spurgeon, S.K. (1998), Sliding Mode Control: Theory and Applications, Taylor & Francis, London, UK.
- Misawa, E.A. and Hedrick, J.K. (1989), "Nonlinear Observers – A State-of-the-Art Survey," Transactions of the ASME, 111, 3, 344-352.
- Bevly, D.M. and Parkinson, B. (2007), "Cascaded Kalman Filters for Accurate Estimation of Multiple Biases, Dead-Reckoning Navigation, and Full State Feedback Control of Ground Vehicles," IEEE Transactions on Control Systems Technology, 15, 2, 199-208.
- Ashley, C. and MacKellar, K.S. (1985), "The Design of the MIRA Straightline Wet Grip Testing Facility," in Proc. of the IMECHE Conference on Anti-Lock Braking Systems for Road Vehicles, 187-197.
- Kiencke, U. and Nielsen, L. (2000), Automotive Control Systems, SAE International, Springer-Verlag, Heidelberg, Germany.